INTERNATIONAL JOURNAL OF PHARMACEUTICAL SCIENCES
[ISSN: 0975-4725; CODEN(USA): IJPS00]
Journal Homepage: https://www.ijpsjournal.com

OPEN ACCESS

Review Paper

pH-Responsive Hydrogels for Oral Colon-Targeted Delivery of Biologics: Recent Advances

Gautami Gangurde*, Dr. Anil Jadhav, Dr. Atul Bendale, Prajwal Aher

SEMS Mahavir Institute of Pharmacy, Nashik.

ARTICLE INFO

Published: 03 July 2026
Keywords:
pH-responsive hydrogels; colon drug delivery; IBD; monoclonal antibodies; siRNA; exosomes; alginate; chitosan; Eudragit; Donnan osmotic swelling; Flory-Rehner theory; Korsmeyer-Peppas; mesh size; mucoadhesion; oral biologic delivery.
DOI:
10.5281/zenodo.21156827

ABSTRACT

Colonic diseases — inflammatory bowel disease, colorectal malignancy, and infectious colitis — require targeted pharmacological intervention at the large intestinal mucosa. Biologic therapeutics such as monoclonal antibodies, recombinant proteins, nucleic acid-based therapies, and extracellular vesicles possess excellent target specificity but face near-complete oral bioavailability failure owing to the sequential degradation imposed by the gastrointestinal tract: acid-mediated unfolding, enzymatic proteolysis, mucus barrier entrapment, and epithelial tight junction restriction. pH-responsive hydrogels exploit the predictable rise in intraluminal pH from the stomach (pH 1.2–2.0) to the ileocolonic junction (pH 6.8–7.4) to achieve site-selective colonic biologic release. These ionisable, crosslinked polymer networks remain structurally compact and protective under acidic gastric conditions, then undergo thermodynamically driven swelling through Donnan osmotic pressure generation and electrostatic repulsion upon carboxylate group ionisation at colonic pH, enabling controlled macromolecular diffusion. This comprehensive review covers the mechanistic basis of pH-responsive swelling from thermodynamic and kinetic perspectives — including Flory-Rehner theory, Donnan osmotic swelling, mesh size dynamics, and Korsmeyer-Peppas drug release modelling — alongside polymer chemistry, formulation design, figure-based schematic analysis, and clinical translation. Ten summary tables and multiple schematic figure descriptions organise GI environmental parameters, polymer benchmarks, swelling thermodynamics, drug release kinetics, biologic delivery outcomes, fabrication approaches, crosslinking strategies, characterisation methods, clinical evidence, and translational challenge-solution pairings

INTRODUCTION

The colonic mucosa holds a dual therapeutic significance rarely encountered in any other organ:

***Corresponding Author:** Gautami Gangurde
Address: *SEMS Mahavir Institute of Pharmacy, Nashik.*
Email ✉: gautamigangurde2003@gmail.com
Relevant conflicts of interest/financial disclosures: The authors declare that the research was conducted in the absence of any commercial or financial relationships that could be construed as a potential conflict of interest.

it is simultaneously the primary site of pathological injury in inflammatory bowel disease and a critical anatomical target for loco-regional gene-based therapies in colorectal carcinoma. This convergence has driven decades of pharmaceutical research into colon-targeted drug delivery systems, yet the reliable and efficient delivery of intact biologic drugs to this site through oral administration remains among the most technically demanding problems in contemporary pharmaceutical science.

Biologic medicines — monoclonal antibodies, recombinant cytokines, small interfering RNA, and mesenchymal stem cell-derived extracellular vesicles — have fundamentally changed the treatment landscape for moderate-to-severe IBD since infliximab entered clinical practice in 1998. Successive generations of anti-TNF-α, anti-integrin, anti-IL-12/23, and JAK-inhibitor agents have progressively expanded the therapeutic armamentarium, achieving mucosal healing rates previously unattainable. Yet these agents all share a pharmacological paradox: systemic administration is required for a disease whose pathological activity is concentrated within the colonic mucosa. High circulating drug concentrations needed to saturate mucosal receptors simultaneously suppress systemic immune surveillance, elevating risks of opportunistic infections, lymphoma, and demyelinating disorders.

pH-responsive hydrogels capitalise on a fundamental physiological asset — the predictable longitudinal pH gradient of the gastrointestinal tract. Anionic polymer networks bearing ionisable carboxylic acid groups remain protonated, compact, and structurally protective throughout the acidic gastric and upper intestinal environment, then undergo progressive ionisation-driven swelling as luminal pH rises toward the ileocolonic junction value of approximately 6.8–7.4. The resulting network expansion enables controlled diffusion of encapsulated biologic payload at the desired colonic target without requiring any external physical, chemical, or electronic triggering mechanism. This review provides a comprehensive, mechanistically deep, and clinically contextualised synthesis of the field, incorporating ten summary tables and detailed schematic figure descriptions.

2. Gastrointestinal Physiology and Pathological Microenvironment

2.1 Longitudinal pH Profile and Its Pharmacological Significance

A thorough understanding of luminal pH values, their variability, and their biological consequences at each gastrointestinal segment is essential for rational pH-responsive hydrogel design. Table 1 consolidates these parameters.

Table 1. Intraluminal pH, transit characteristics, and drug delivery significance at successive gastrointestinal anatomical regions.

Anatomical Region	Luminal pH	Residence Duration	Delivery Design Implications
Stomach (fasted)	1.2–2.0	0.5–2 h	Outer hydrogel must withstand acid; biologic at risk of unfolding below pH 3.0
Stomach (postprandial)	3.0–5.0	1–4 h	Food transiently buffers acid; enteric coatings may partially swell; robust second barrier needed

Duodenum	5.5–6.5	15–30 min	Pancreatic proteases active; L100-55 dissolution threshold reached; S100 still intact
Jejunum / Ileum	6.5–7.2	2–4 h	Brush-border peptidases active; L100 may begin dissolving; S100 coat remains protective
Ileocaecal junction	6.8–7.4	Variable	Primary trigger zone for S100 dissolution and anionic hydrogel swelling onset
Ascending/transverse colon	6.5–7.5	6–24 h	Highest microbial density; ROS elevated in IBD; extended transit supports prolonged biologic release
Sigmoid/descending colon	7.0–8.0	Up to 48 h	Highest pH; complete enteric coat dissolution; suitable for sustained colonic biologic release

Gastric pH in the fasted adult ranges from 1.2 to 2.0, generated by parietal cell H^+/K^+-ATPase proton secretion. This highly acidic milieu constitutes the primary threat to biologic integrity, as most globular proteins undergo irreversible tertiary structure collapse below pH 3.0 through protonation of buried histidine, aspartate, and glutamate residues that normally stabilise the hydrophobic core. RNA molecules undergo acid-catalysed hydrolysis of the phosphodiester backbone with a half-life measured in seconds at pH 1.2. Upon pyloric evacuation, pancreatic bicarbonate secretion raises duodenal pH to 5.5–6.5 within minutes; jejunal and ileal pH progresses to 6.5–7.2. The ileocaecal junction, where pH reaches 6.8–7.4, represents the pharmacologically defined trigger zone for colonic delivery systems. Clinically significant variability arises from proton pump inhibitor therapy, achlorhydria, and active IBD-associated lactic acid accumulation in the inflamed colonic mucosa.

2.2 IBD Pathological Microenvironment

Active IBD creates a distinctive colonic microenvironment that differs from healthy tissue across multiple physicochemically relevant dimensions. Activated neutrophils and macrophages generate reactive oxygen species — principally H_2O_2, superoxide ($O_2^{\bullet -}$), and hypochlorite (HOCl) — at concentrations 10- to 100-fold above healthy mucosal baselines through NADPH oxidase-mediated pathways. This elevated ROS burden simultaneously constitutes a therapeutic target and a secondary formulation trigger for dual pH/ROS-responsive carriers. Mucosal permeability is pathologically increased through redistribution of claudin-1, occludin, and ZO-1 tight junction proteins, creating paracellular gaps that may paradoxically facilitate macromolecular absorption from colonic lumen to submucosal compartment — a feature exploited by site-selective biologic delivery systems. IBD dysbiosis reduces populations of polysaccharide-degrading Bacteroidetes, compromising the enzymatic lability of pectin and guar gum matrices that rely on microbial pectinase and galactomannanase for colonic release.

3. Mechanisms of pH-Responsive Swelling and Drug Release

Understanding the mechanistic basis of pH-triggered swelling and drug release in hydrogel systems is fundamental to rational formulation design at the M.Pharm level. The release

behaviour of pH-responsive hydrogels is governed by a sequence of interconnected thermodynamic, electrostatic, and kinetic phenomena that collectively determine the magnitude, rate, and selectivity of biologic payload liberation at the target GI site.

3.1 Thermodynamic Framework: Flory-Rehner Theory

The equilibrium swelling behaviour of a crosslinked polymer network in a solvent is described by the Flory-Rehner theory, which recognises two opposing contributions to the total free energy of swelling. The first is the free energy of mixing (ΔGmix), which is negative (favourable) when the polymer-solvent interaction parameter χ (Flory-Huggins parameter) is sufficiently low — this thermodynamic component drives the polymer to absorb solvent. The second is the elastic free energy of the crosslinked network (ΔGelastic), which is positive (unfavourable) because swelling stretches the polymer chains between crosslinks, storing elastic energy analogous to a mechanical spring. At equilibrium swelling, these two contributions exactly balance:

$\Delta G_{total} = \Delta G_{mix} + \Delta G_{elastic} = 0$

For pH-responsive anionic hydrogels, the critical insight is that ionisation of carboxylic acid groups above their pKa dramatically lowers the effective χ parameter by introducing electrostatic repulsion between adjacent polymer chain segments — repulsion that the Flory-Huggins model treats as an additional driving force for chain expansion. The Flory-Rehner equation for the equilibrium polymer volume fraction in the swollen network ($v_{2,s}$) — which is inversely proportional to the degree of swelling — is given by:

$$[\ln(1 - v_{2,s}) + v_{2,s} + \chi v_{2,s}^2] + V_1/V_c \times (v_{2,s}^{1/3} - v_{2,s}/2) = 0$$

where V_1 is the molar volume of the solvent and V_c is the molar volume of the polymer between crosslinks. At gastric pH, carboxylate groups are protonated (R-COOH), χ remains high, and $v_{2,s}$ is large (low swelling — compact network). At colonic pH (above pKa), progressive deprotonation generates $R\text{-}COO^-$ anions, electrostatic repulsion lowers effective χ, and $v_{2,s}$ falls dramatically — corresponding to large-scale swelling. The mesh size (ξ) of the swollen network, which governs the diffusion of encapsulated biologic molecules, scales with $v_{2,s}$ according to:

$$\xi = v_{2,s}^{-1/3} \times (\bar{r}0^2)^{1/2}$$

where $\bar{r}0$ is the root-mean-square end-to-end distance of the freely jointed polymer chain between crosslinks. For a biologic with hydrodynamic radius rs to diffuse through the network, ξ must exceed rs. For IgG antibodies (rs ≈ 5–8 nm), ξ must reach approximately 10 nm at colonic pH — a design criterion that directly specifies the required crosslink density.

[FIGURE 1 — Schematic of pH-Triggered Swelling Mechanism]

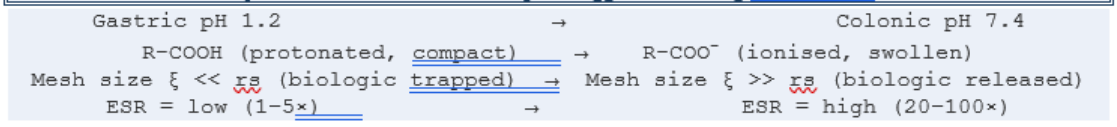

Figure 1. Schematic representation of pH-triggered swelling in anionic hydrogels. At gastric pH, carboxylic acid groups remain protonated (R-COOH), maintaining a compact network with mesh size smaller than the biologic hydrodynamic radius. Upon reaching colonic pH, ionisation generates fixed negative charges ($R\text{-}COO^-$), electrostatic repulsion drives rapid water uptake and network expansion, and mesh size exceeds the critical threshold for macromolecular diffusion. ESR = equilibrium swelling ratio. The double arrows indicate the reversibility of the swelling transition — relevant to self-healing Schiff base hydrogels — while the one-way arrow indicates the physiological context of irreversible transit toward the colon.

3.2 Donnan Osmotic Pressure and Electrostatic Swelling Driving Force

The Donnan membrane equilibrium provides the quantitative electrostatic framework for understanding swelling in ionisable hydrogels. When a polyelectrolyte hydrogel bearing fixed charges (ionised carboxylate groups, R-COO$^-$) is immersed in an electrolyte solution, mobile counterions (primarily Na^+) are preferentially concentrated within the gel interior relative to the external solution, while mobile co-ions (Cl^-) are excluded by electrostatic repulsion. This unequal ion distribution creates a Donnan osmotic pressure (π) across the gel-solution interface, which drives water into the hydrogel network:

$\pi = RT \times \Sigma i\ (ci,gel - ci,solution)$

where ci,gel and ci,solution are the molar concentrations of mobile ion species i inside and outside the gel, R is the gas constant, and T is absolute temperature. At gastric pH, where carboxylate groups are protonated, there are no fixed charges, no Donnan effect, and no osmotic swelling driving force beyond simple polymer-solvent mixing — explaining why anionic hydrogels remain compact in the stomach. As pH rises above the polymer pKa at the ileocolonic junction, progressive deprotonation introduces fixed negative charges, the Donnan potential increases, counterion concentration gradient between gel interior and external GI fluid grows, and osmotic water influx drives dramatic network expansion.

The magnitude of Donnan swelling depends critically on the degree of ionisation (α), which is governed by the Henderson-Hasselbalch relationship:

$\alpha = 1 / (1 + 10^{(pKa - pH)})$

At colonic pH 7.4, a polymer with pKa 3.5 (e.g., alginate carboxylates) exhibits $\alpha \approx 1.0$ (essentially complete ionisation), while at gastric pH 1.2, $\alpha \approx 10^{-2.3}$ (< 1% ionisation). This sharp ionisation transition across the GI pH gradient translates directly into the dramatic swelling selectivity that makes anionic hydrogels effective colonic delivery vehicles. For polymer systems with pKa values in the range of 4.5–6.0 (e.g., PAA, Carbopol), partial ionisation begins in the jejunum (pH 6.5) — explaining the tendency toward premature small intestinal swelling with these materials and the rationale for using Eudragit® S100 (which dissolves only above pH 7.0) as an outer coating to delay swelling onset.

[FIGURE 2 — Donnan Osmotic Pressure and Degree of Ionisation vs. GI pH]

Degree of Ionisation (α) vs. Luminal pH

	pH: 1.2	2.0	4.5	6.0	6.8	7.4	8.0	
α(3.5):	0%	0%	9%	100%	100%	100%	100%	← Alginate / Pectin
α(5.0):	0%	0%	9%	50%	97%	100%	100%	← PAA / Carbopol
S100:	stable	stable	stable	stable	stable	dissolve	dissolve	← Eudragit S100

Figure 2. Degree of ionisation (α) of key anionic polymers as a function of gastrointestinal luminal pH, calculated using the Henderson-Hasselbalch equation. Alginate and pectin (pKa ~3.4–3.5) reach near-complete ionisation by duodenal pH but their Ca^{2+}-crosslinked networks rely on ionic stability rather than protonation to maintain integrity. PAA/Carbopol (pKa ~5.0) shows partial ionisation (50%) in the jejunum, explaining premature swelling tendency. Eudragit® S100 undergoes film dissolution — not ionisation-driven swelling — above pH 7.0, providing the most selective colonic trigger among clinically established materials.

3.3 Mesh Size Dynamics and Macromolecular Diffusion

The mesh size (ξ) of a swollen hydrogel network is the single most critical structural parameter governing whether an encapsulated biologic can

diffuse through the matrix. It can be estimated from the Flory-Rehner equation or from mechanical data using the rubber elasticity theory:

$\xi = (RT / G')^{(1/3)} \times v_{2,s}^{(-1/3)}$

where G' is the storage modulus measured by oscillatory rheology and $v_{2,s}$ is the polymer volume fraction in the swollen state. The effective diffusion coefficient of a spherical biologic molecule with Stokes radius rs through the hydrogel network is described by the Ogston-type hindered diffusion model:

$D_{eff} / D_0 = \exp(-\pi \times r_s^2 / \xi^2)$

This exponential dependence on $(r_s/\xi)^2$ has profound practical consequences: even a modest increase in mesh size from pH-triggered swelling produces a large amplification in biologic diffusivity. For example, if ξ increases from 4 nm (gastric pH) to 12 nm (colonic pH) — a 3-fold change — and rs for a 30 kDa protein is 2 nm, then Deff/D0 increases from $\exp(-\pi \times 4/16) \approx 0.46$ to $\exp(-\pi \times 4/144) \approx 0.92$, nearly doubling the fractional diffusivity. For IgG antibodies (rs ≈ 7 nm), the same mesh expansion switches the system from essentially impermeable ($D_{eff}/D_0 \approx \exp(-\pi \times 49/16) \approx 0.000055$) to moderately permeable ($D_{eff}/D_0 \approx \exp(-\pi \times 49/144) \approx 0.34$) — a 6,000-fold increase in effective diffusivity, explaining the dramatic pH-sensitivity of biologic release from well-designed hydrogel systems.

3.4 Drug Release Kinetic Models

Following pH-triggered swelling and network expansion, the kinetics of biologic payload release from the hydrogel matrix are described by a hierarchy of mathematical models of increasing mechanistic complexity. Selection of the appropriate model — based on goodness of fit ($r^2 > 0.99$) and mechanistic plausibility — is an important component of hydrogel formulation characterisation at the M.Pharm level. Table 9 summarises the principal kinetic models with their equations, mechanistic interpretations, and specific relevance to pH-responsive hydrogel systems.

Table 9. Mathematical models for drug release kinetics from pH-responsive hydrogels, with mechanistic interpretations and hydrogel-specific relevance.

Kinetic Model	Mathematical Equation	Release Mechanism	Relevance for pH-Responsive Hydrogels
Zero-order	$Q_t = Q_0 + K_0 t$	Constant rate; independent of concentration	Applicable to matrix systems releasing biologic at constant rate after pH-triggered swelling plateau; rarely achieved alone in swellable hydrogels
First-order	$\log Q_t = \log Q_0 - K_1 t / 2.303$	Rate proportional to remaining drug concentration	Governs early burst release of surface-adsorbed biologic from hydrogel before swelling equilibrium; common in alginate bead systems
Higuchi model	$Q_t = K_H \sqrt{t}$	Diffusion-controlled from matrix	Describes protein diffusion from swollen hydrogel matrix post pH-trigger; applicable when mesh size >> biologic hydrodynamic radius

Korsmeyer-Peppas	Mt/M∞ = Ktn	n ≤ 0.45: Fickian diffusion; 0.45 < n < 0.89: anomalous; n = 0.89: Case-II (swelling-controlled); n > 0.89: Super Case-II	Most widely applied to pH-responsive hydrogels; n value distinguishes diffusion- vs swelling-dominated release; biologic macromolecules typically show anomalous (non-Fickian) transport due to coupled swelling and diffusion
Peppas-Sahlin	Mt/M∞ = K1tm + K2t2m	Separates Fickian diffusion (K1 term) from relaxation/swelling contribution (K2 term)	Particularly useful for pH-responsive hydrogels where network relaxation (swelling-driven chain mobility changes) and molecular diffusion simultaneously govern release; K2/K1 ratio quantifies relative contribution of each mechanism
Hixson-Crowell	Q0^(1/3) − Qt^(1/3) = Kst	Surface area-controlled erosion/dissolution	Applicable to Eudragit® S100-coated systems where pH-triggered outer coating dissolution controls total surface area available for drug release; erosion-dominant mechanism

The Korsmeyer-Peppas power law model (Mt/M∞ = Ktn) is the most widely applied kinetic framework for pH-responsive hydrogels because the diffusion exponent n directly distinguishes the dominant release mechanism without requiring knowledge of the diffusion coefficient or network geometry. For slab geometry — the relevant geometry for film-coated tablets and flat hydrogel matrices — n = 0.5 indicates Fickian diffusion (biologic concentration-gradient-driven), n = 1.0 indicates Case-II transport (swelling-rate-controlled, zero-order release), and 0.5 < n < 1.0 indicates anomalous (non-Fickian) transport where both diffusion and network swelling contribute to release. For biologic macromolecules with large hydrodynamic radii, anomalous transport (n values of 0.6–0.85) is the most commonly reported mechanism in pH-responsive alginate, chitosan, and PAA-based systems — consistent with the coupled swelling and diffusion processes governing their release. For cylindrical beads and spherical particles (the most common morphologies for oral colonic formulations), the critical n values shift to 0.45 (Fickian) and 0.89 (Case-II), and the Korsmeyer-Peppas equation is typically applied to only the first 60% of cumulative release (Mt/M∞ ≤ 0.60) to avoid artefacts from the late-phase depletion of drug reservoir.

The Peppas-Sahlin model, which deconvolutes total release into a pure Fickian diffusion term ($K_1 \times t^m$) and a pure swelling relaxation term ($K_2 \times t^{2m}$), is particularly informative for pH-responsive hydrogels where network relaxation — the time-dependent conformational rearrangement of polymer chains upon swelling — is an important kinetic process. The ratio K_2/K_1 quantifies the relative contribution of swelling-driven (Case-II) transport versus concentration-gradient-driven Fickian diffusion; a high K_2/K_1 ratio (> 1) identifies formulations where the rate of network swelling, rather than biologic diffusivity, is the rate-limiting step for payload release.

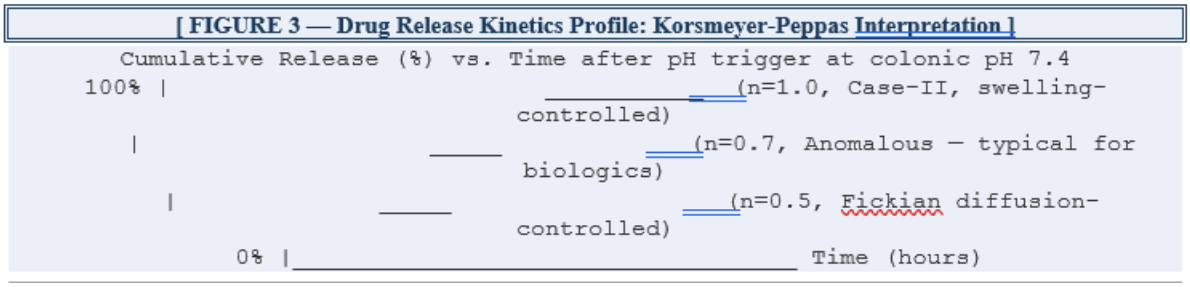

Figure 3. Schematic drug release profiles illustrating Korsmeyer-Peppas diffusion exponent interpretation for pH-responsive hydrogels at colonic pH (pH 7.4 trigger). n = 0.5 (Fickian) indicates biologic release is driven solely by concentration gradient diffusion through a stable swollen network; n = 0.7 (anomalous) represents the most common case for biologic macromolecules where coupled swelling and diffusion operate simultaneously; n = 1.0 (Case-II) indicates network swelling rate is rate-limiting, producing near-zero-order release. For IgG antibodies in alginate/chitosan systems, reported n values typically fall between 0.6 and 0.85.

3.5 Swelling Thermodynamics Summary

Table 10 consolidates the key thermodynamic and kinetic parameters governing pH-responsive hydrogel swelling and biologic release, providing a structured reference for formulation design decisions.

Table 10. Thermodynamic and kinetic parameters governing pH-responsive hydrogel swelling and macromolecular biologic release.

Theoretical Parameter	Definition / Equation	Physical Significance	Impact on Biologic Release
Equilibrium swelling ratio (ESR)	ESR = (Ws − Wd) / Wd Ws = swollen mass; Wd = dry mass	Quantifies total water uptake; reflects ionisation extent and osmotic driving force at given pH	Higher ESR → larger mesh size → faster macromolecular diffusion; ESR ratio pH 7.4/1.2 defines trigger selectivity
Polymer volume fraction (v2,s)	v2,s = Vd / Vs Vd = dry volume; Vs = swollen volume	Inversely proportional to swelling; decreases as crosslink density falls or ionisation increases	Low v2,s (high swelling) increases mesh size; must not fall below threshold that causes biologic leaching before target site
Flory-Rehner mesh size (ξ)	ξ = v2,s^(−1/3) × (r̄0²)^(1/2) r̄0 = end-to-end distance of polymer chain	Average pore diameter of swollen network; determines steric accessibility of biologic payload	For IgG delivery: ξ must exceed ~10 nm (IgG hydrodynamic diameter) at colonic pH while remaining <5 nm at gastric pH to prevent premature release
Flory-Huggins interaction parameter (χ)	χ = Vs/RT × (δs − δp)² δs, δp = solubility parameters of solvent and polymer	Quantifies polymer-solvent thermodynamic compatibility; lower χ =	Anionic polymers exhibit lower effective χ above pKa

		better swelling thermodynamics	due to electrostatic repulsion amplifying thermodynamic swelling driving force at colonic pH
Donnan osmotic pressure (π)	$\pi = RT \times \Sigma(ci,in - ci,out)$ ci = ion concentration inside/outside gel	Osmotic pressure generated by fixed charges on ionised polymer chains retaining mobile counterions; major swelling driving force above pKa	At colonic pH, ionised carboxylate groups accumulate Na^+ counterions within network; resulting osmotic gradient drives water influx, rapid mesh expansion, and accelerated biologic diffusion
Effective diffusion coefficient (Deff)	$Deff = D0 \times \exp(-\pi \times rs^2 / \xi^2)$ D0 = free solution diffusivity; rs = solute radius	Actual diffusivity of biologic through swollen hydrogel network; strongly dependent on ratio of solute radius to mesh size	Exponential dependence means small increases in mesh size (from pH-triggered swelling) produce large increases in biologic diffusion coefficient; explains rapid release onset at trigger pH

3.6 Polymer-Specific pH-Response Mechanisms

3.6.1 Alginate: Ionotropic Gelation and pH-Triggered Decrosslinking

Sodium alginate forms physical hydrogel networks through cooperative coordination of Ca^{2+} ions with the carboxylate groups of guluronate (G-block) sequences in an antiparallel pairing arrangement — the egg-box model. At gastric pH, the Ca^{2+}-guluronate coordination bonds are supplemented by protonation of carboxylate groups, which reduces electrostatic repulsion between chains and stabilises the junction zones. As luminal pH rises through the small intestine, progressive deprotonation of the mannuronate and guluronate carboxylates (pKa ~3.4) increases electrostatic repulsion within and between polymer chains, weakening junction zones. However, the Ca^{2+} coordination itself provides substantial structural integrity independent of protonation state — explaining why alginate beads frequently require phosphate ion-mediated Ca^{2+} chelation (which disrupts junction zones by competing for Ca^{2+}) in addition to pH-triggered carboxylate ionisation for complete dissolution in the small intestine. This is the mechanism by which phosphate-buffered simulated intestinal fluid (SIF-USP) challenges alginate matrix integrity — and why Eudragit® S100 outer coating or chitosan inner layers are added to protect against premature SIF-induced dissolution.

3.6.2 Eudragit S100: Anionic Copolymer Dissolution Above pH 7.0

Eudragit® S100 is a random copolymer of methacrylic acid (MAA) and methyl methacrylate (MMA) in a 1:2 molar ratio. The MAA repeat units

bear carboxylic acid groups with an apparent pKa of approximately 6.8–7.0 — shifted upward from the free acid value (~4.6) by the hydrophobic MMA microenvironment and the polyelectrolyte effect. Below pH 7.0, the MAA units are predominantly protonated, and the MMA hydrophobic segments maintain the polymer in a glassy, water-impermeable film state. Above pH 7.0, sufficient carboxylate ionisation occurs to generate electrostatic repulsion between chain segments and osmotic water influx into the film, leading to rapid film dissolution. The sharp dissolution threshold at pH 7.0 — experimentally confirmed by the absence of significant drug release below pH 6.8 in well-formulated Eudragit S100-coated systems — makes this polymer the most reliable pH trigger for ileocolonic targeting currently available.

3.6.3 Chitosan: Cationic pH Response and Polyelectrolyte Complex Behaviour

Chitosan's primary amine groups (pKa 6.2–6.5) protonate at acidic pH, making the polymer cationic, soluble, and swollen. At neutral-to-alkaline colonic pH, deprotonation causes chitosan to collapse and precipitate from solution. This inverse pH response is leveraged in polyelectrolyte complex (PEC) formation with anionic polymers such as alginate: the electrostatic pairing between alginate carboxylates ($R\text{-}COO^-$) and chitosan ammonium groups ($R\text{-}NH_3^+$) creates a stable polyelectrolyte complex that is resistant to dissolution across a wide pH range. As pH rises above 7.0 at the ileocolonic junction, two concurrent changes destabilise the PEC: (i) alginate carboxylate groups become fully ionised, generating repulsion that disrupts chain pairing; and (ii) chitosan amine groups begin deprotonating (above pKa 6.2), reducing the cationic charge density available for electrostatic pairing. The combination of these two effects produces a sharp dissolution transition at the ileocolonic pH — which is the mechanistic basis for the superior colon-selectivity of alginate-chitosan composite hydrogel beads compared to single-polymer systems.

4. pH-Responsive Polymers: Chemistry and Biologic Suitability

Polymer selection is the foundational formulation decision governing release threshold, network stability, biologic compatibility, and regulatory acceptability. Table 2 provides a comparative overview of the major polymer classes.

Table 2. Comparative properties of major pH-responsive polymers employed in colon-targeted biologic delivery hydrogels.

Polymer	Origin	Trigger pH	Swelling at pH 7.4	Principal Strengths	Notable Limitations
Sodium alginate	Natural, anionic	pKa ~3.4	Very high (~99% water)	Aqueous Ca^{2+} gelation; no solvent risk; biodegradable	Phosphate-mediated premature dissolution; M/G batch variability
Chitosan (native)	Natural, cationic	pKa ~6.2–6.5	Collapses at neutral pH	Strong mucoadhesion; tight junction modulator; amine-rich for grafting	Inverse pH response; must be blended for colon release
Pectin (LM)	Natural, anionic	pKa ~3.5	Moderate–high	Dual pH + pectinase	Dysbiotic IBD microbiome may

				enzymatic trigger; selective colonic degradation	reduce enzymatic reliability
CMGG (modified guar)	Semi-synthetic	~4.5	High post-modification	Galactomannanase lability; low cost; non-immunogenic	pH-insensitive until modified; limited biologic loading data
Hyaluronic acid	Natural, anionic	pKa ~3.0	High (crosslinked)	CD44-receptor targeting of inflamed macrophages; ECM-mimetic	Rapid hyaluronidase degradation; requires crosslinking
Eudragit® S100	Synthetic, anionic	Dissolves ≥pH 7.0	Film dissolution	Clinically established; precise pH threshold; regulatory precedent	Coating only; must combine with inner hydrogel for rate control
Poly(acrylic acid)/Carbopol	Synthetic, anionic	pKa ~4.5–5.0	50–100× swelling	Extreme swelling ratio; strong mucoadhesion; well characterised	Premature jejunal swelling at pH 6.5; synthetic origin
IAc–AAm nanogel	Synthetic	pKa ~2.9/~5.5	~10× vs gastric	Intrinsic ROS scavenging (5× control); dual-function therapeutic + responsive	Limited long-term toxicology; scalability unproven

4.1 Natural Polysaccharides

Sodium alginate forms Ca^{2+}-crosslinked beads under entirely aqueous, ambient-temperature conditions that impose minimal stress on co-encapsulated biologics. Encapsulation efficiency for model proteins via in situ gelation routinely exceeds 80%, with preserved biological activity after simulated gastric exposure documented in alginate-chitosan nanosphere systems. Chitosan, the only naturally derived cationic polysaccharide in broad pharmaceutical use, contributes mucoadhesion through electrostatic attraction to negatively charged mucin glycoproteins, paracellular tight junction opening through ZO-1 redistribution, and versatile chemical modification capacity. Thiolated chitosan forms disulfide bonds with mucin cysteine residues for covalent mucoadhesion of substantially greater duration than electrostatic attachment. Pectin provides dual-mechanism colon selectivity through pH-triggered swelling and selective pectinase degradation by colonic Bacteroidetes. Hyaluronic acid adds active CD44-receptor targeting to pH-triggered passive release, concentrating biologic delivery in inflamed macrophages and tumour cells.

4.2 Synthetic pH-Responsive Polymers

Eudragit® S100 occupies a unique position as the only pH-responsive polymer with documented regulatory approval history for colon-targeted delivery, its dissolution threshold at pH ≥7.0

providing a reliable trigger aligned with the ileocolonic junction. Crosslinked polyacrylic acid (Carbopol®) delivers the most dramatic swelling responses — 50- to 100-fold increase from gastric to intestinal pH — at the cost of swelling onset at jejunal pH (6.5), addressed by copolymerisation with hydrophobic monomers or IPN formation with enzymatically labile polysaccharides. Itaconic acid-acrylamide nanogels represent a multifunctional advance: pH-responsive swelling (10-fold between gastric and colonic pH) combined with intrinsic ROS-scavenging activity five times greater than control materials.

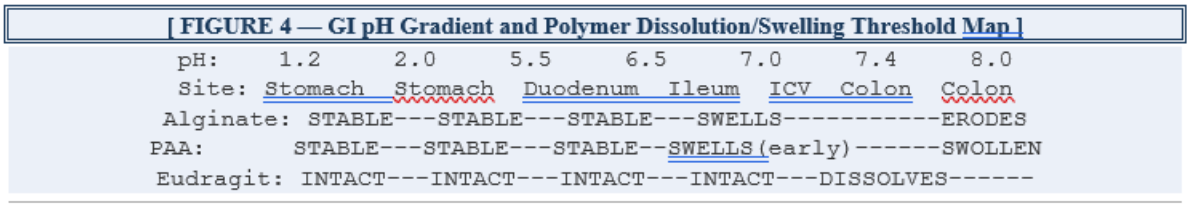

Figure 4. Schematic map of pH-responsive polymer behaviour across the gastrointestinal pH gradient. ICV = ileocaecal valve. Alginate swells at ileocolonic pH but may dissolve prematurely in phosphate-rich simulated intestinal fluid without outer coating protection. PAA/Carbopol begins swelling at jejunal pH (6.5), indicating risk of small intestinal biologic release. Eudragit® S100 remains intact as a film until pH 7.0 is reached at the ileocaecal valve, providing the most selective colonic trigger. Combining an Eudragit® S100 outer coat with an inner alginate hydrogel reservoir exploits the complementary properties of both systems.

5. Formulation Architecture, Crosslinking, and Biologic Loading

5.1 Crosslinking Strategy Comparison

The crosslinking strategy shapes every downstream performance characteristic. Table 6 provides a structured comparison.

Table 6. Comparison of crosslinking strategies for pH-responsive hydrogels used in colon-targeted biologic delivery.

Crosslinking Type	Example Chemistry	Gel Stability	Biologic Safety Profile	pH-Release Mechanism
Ionotropic (physical)	Ca^{2+} + alginate carboxylates	Moderate; dissolves in phosphate-rich fluid	Excellent — aqueous, room temp, no radicals	Carboxylates protonated at gastric pH; Ca^{2+} displaced by phosphate at intestinal pH
Polyelectrolyte complex	Alginate–chitosan ionic pairing	Good; reinforced by LBL deposition	Excellent — no chemical reagents; aqueous mixing	Anionic component swells as pH rises above pKa; erosion above pH 7.0
Covalent radical (permanent)	MBA or EGDMA + AAm/AAc	High; hydrolytically stable	Moderate — radical intermediates risk Met/Trp oxidation; post-gelation loading needed	Ionisable carboxylates swell mesh above pKa; macromolecular diffusion enabled at colonic pH

Dynamic covalent Schiff base	Oxidised CMC + chitosan amine	Moderate; pH-labile below pH 5	Good — gelation at physiological pH/temp; self-healing; injectable	Imine bonds hydrolyse at acidic pH; reform at neutral pH; net release by GI pH cycling
Boronate ester (pH + ROS)	Phenylboronic acid + cis-diol polymer	Moderate; dual trigger required	Good — aqueous crosslinking; dissolves only when both pH and ROS thresholds exceeded	Boronate ester hydrolysed by acidic pH or H_2O_2; dual-trigger maximises colon specificity
Photocrosslinking (UV)	Methacrylated HA/GelMA + photoinitiator	High; stable under GI conditions	Moderate — low initiator conc limits radical exposure; far-UV risks nucleic acid damage	Ionisable groups swell at colonic pH; crosslink density tuneable by irradiation dose

Physical crosslinks — ionotropic Ca^{2+} coordination, polyelectrolyte pairing, hydrogen bonding — are inherently reversible and pH-sensitive. Boronate ester crosslinks are particularly attractive for dual-responsive colon targeting because they are hydrolysed by both acidic pH and H_2O_2, enabling disease-selective release in IBD tissue characterised by both near-neutral pH and elevated ROS.

5.2 Biologic Loading and Multilayer Architecture

Biologic loading strategy must be matched to molecular weight, charge, and conformational sensitivity of the payload. Table 4 compares fabrication methods and their biologic compatibility.

Table 4. Fabrication methods for pH-responsive hydrogels and their suitability for encapsulating macromolecular biologics.

Method	Compatible Polymers	Size Range	Biologic Compatibility Considerations
Ionotropic gelation	Alginate, pectin, carrageenan	500 µm–3 mm	Excellent: aqueous, mild Ca^{2+} crosslinking at room temp; no radicals; widely used for proteins and antibodies
Electrospray / coaxial	Alginate, chitosan, PVA blends	200 nm–500 µm	Good: tunable size; coaxial configuration isolates biologic core from polymer shell minimising denaturation
Free radical polymerisation	PAA, Carbopol, IAc-AAm	10 nm–1 µm	Moderate: radical species risk protein oxidation; post-gelation loading with radical scavengers recommended
Layer-by-layer (LBL)	Alginate/chitosan + Eudragit coat	1–10 µm	Good: stepwise aqueous deposition; pH threshold tuneable by L100:S100 ratio; validated for protein-loaded beads

Schiff base gelation	Oxidised CMC + modified chitosan	Injectable bulk gel	Good: gelation within 30–120 s at physiological temperature; self-healing; no external crosslinker required
Nanoparticle-in-hydrogel	Alginate/HA + LNP/MOF/PLGA NPs	Macrogel + 50–500 nm NPs	Excellent for RNA: dual protection — NP shields siRNA/mRNA from nucleases; hydrogel absorbs acid and mechanical stress
Spray-freeze-drying	Eudragit, HPMC, alginate matrices	1–200 µm	Moderate-good: sub-ambient processing avoids heat denaturation; lyoprotectant selection critical; preferred over spray-drying for biologics

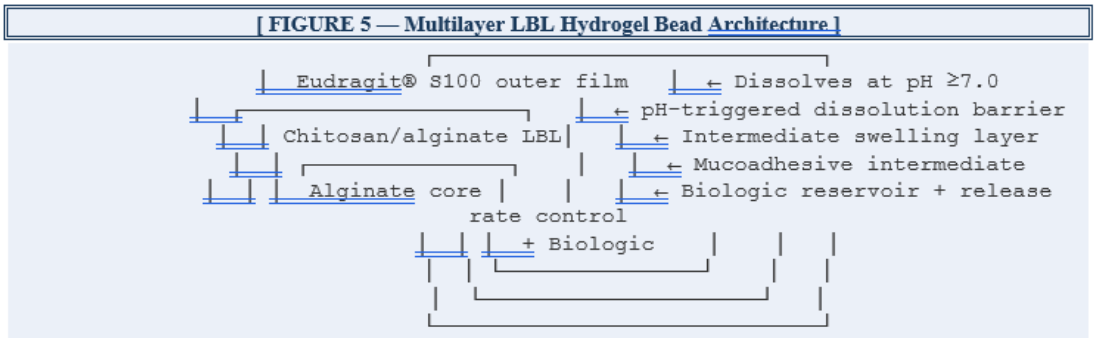

Figure 5. Cross-sectional schematic of a multilayer layer-by-layer (LBL) hydrogel bead for colon-targeted biologic delivery. The innermost alginate core serves as the biologic reservoir and primary release-rate-control domain; mesh size at gastric pH prevents biologic diffusion while swelling at colonic pH enables release. The intermediate chitosan/alginate LBL bilayers (typically 3–10 bilayers) provide additional mechanical stability, mucoadhesive surface charge, and microbiota enzyme-triggered degradability. The outermost Eudragit® S100 film ensures no payload liberation occurs before pH 7.0 is reached at the ileocaecal junction. Each functional layer is independently optimisable — a key advantage of LBL architecture over single-polymer systems.

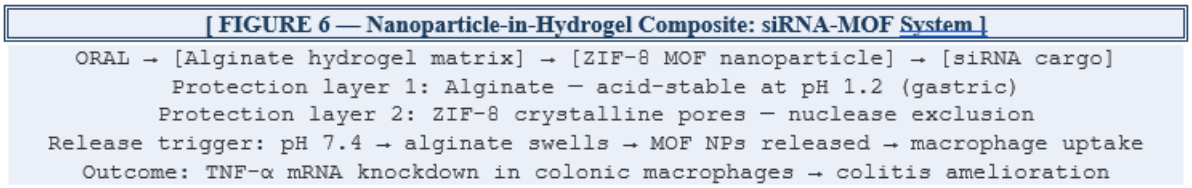

Figure 6. Sequential protection architecture of the alginate–ZIF-8 MOF nanoparticle composite for oral siRNA delivery to the colon. ZIF-8 (zeolitic imidazolate framework-8) is a metal-organic framework formed by zinc ions coordinating with 2-methylimidazolate linkers, producing a crystalline porous structure with pore apertures of approximately 3.4 Å — small enough to exclude RNase A (hydrodynamic radius ~19 Å) while accommodating siRNA condensation through electrostatic interaction with zinc nodes. The surrounding sodium alginate hydrogel matrix provides acid stability at gastric pH through compact network maintenance and absorbs mechanical GI transit forces. At colonic pH, alginate swells and releases MOF nanoparticles, which are internalised by mucosal macrophages through endocytosis, with subsequent endosomal escape enabling cytoplasmic siRNA delivery and RISC-mediated mRNA silencing.

6. Recent Advances by Biologic Class

Table 3 consolidates recent documented outcomes for pH-responsive hydrogel systems evaluated for specific biologic payloads.

Table 3. Selected recent reports of pH-responsive hydrogel systems evaluated for colon-targeted biologic delivery.

Biologic Class	Specific Agent	Hydrogel Platform	Reported Findings	Experimental Model	Ref.
Anti-TNF-α mAb	Infliximab analogue	Folic acid-chitosan clay nanocomposite + pH coat	Preserved IgG structure at pH 1.2 & 6.8; targeted delivery to folate receptor+ macrophages	Caco-2; rat colitis	[17]
Anti-IL-6 mAb	Recombinant anti-IL-6	Amino acid excipient core + pH/enzyme Eudragit coat	Colonic tissue antibody uptake exceeded i.p. injection; IL-6 mRNA downregulation	DSS colitis mouse	[5]
TNF-α Ab + MSC exosomes	Anti-TNF IgG; UMSC-EXOs	Fluidic microgel assembly (FMGA)	48-h mucosal retention; ZO-1/occludin restoration; microbiota diversity recovered	DSS mouse + beagle IBD	[16]
Model protein	BSA (66 kDa)	Alginate/chitosan nanospheres	pH-dependent release; EE >80%; low haemolysis; low Caco-2 cytotoxicity	In vitro	[6]
siRNA (gene silencing)	TNF-α siRNA	Sodium alginate + ZIF-8 MOF-siRNA nanoparticles	Survived gastric acid; colonic accumulation; TNF-α knockdown; colitis amelioration	DSS colitis mouse	[21]
siRNA (sustained)	GFP-targeting siRNA	Gellan gum + DOTAP lipoplexes	60-day controlled release; retained knockdown in DLD1 colon cancer cells	DLD1 CRC in vitro	[22]
ROS-scavenging nanogel	IAc-AAm nanogel	Itaconic acid–acrylamide nanogel (190 nm)	10-fold swelling pH 1.2→7.4; superoxide scavenging 5×	In vitro pH + ROS assays	[3]

			control; cytocompatible		

6.1 Monoclonal Antibodies

Encapsulating anti-IL-6 antibodies in amino acid excipient cores surrounded by Eudragit® coating dissolving at colonic pH demonstrated that colonic tissue antibody concentrations after oral administration exceeded those from intraperitoneal injection at equivalent doses in DSS-induced colitis mice — with correspondingly greater IL-6 mRNA downregulation. Folic acid-grafted clay-chitosan nanocomposites loaded with an infliximab analogue confirmed intact antibody secondary and tertiary structure (CD spectroscopy, SDS-PAGE) after 2-hour simulated gastric exposure and site-selective delivery to folate receptor-expressing macrophages in inflamed colonic mucosa.

6.2 Therapeutic Proteins

Recombinant proteins including BSA (66 kDa), intestinal trefoil factor, and epidermal growth factor have been evaluated in pH-responsive systems with consistent documentation of pH-dependent release favouring liberation at colonic pH. An oral hydrogel nanoemulsion co-delivery system combining alginate/hyaluronic acid matrix achieved biphasic release — immediate burst from nanoemulsion droplets followed by sustained matrix release — with significant anti-inflammatory and barrier restoration outcomes in DSS-colitis models. The HA component provided CD44-mediated macrophage targeting, concentrating the anti-inflammatory payload in the innate immune cells primarily responsible for cytokine-driven mucosal damage.

6.3 siRNA and Exosomes

The alginate–ZIF-8 MOF composite (detailed in Figure 6) achieved survival of gastric acid, preferential colonic accumulation exploiting IBD-enhanced mucosal permeability, significant TNF-α mRNA knockdown, and histopathological colitis improvement. MSC-derived exosomes loaded into fluidic microgel assemblies (FMGAs) achieved 48-hour mucosal retention, restoration of ZO-1, occludin, and claudin-1 tight junction protein expression, and improved gut microbiota diversity in both DSS mouse colitis and a beagle canine IBD model.

7. Emerging Multi-Stimuli Responsive Systems

7.1 Dual pH/ROS Platforms

The pathological co-occurrence of near-neutral pH and markedly elevated ROS in actively inflamed colonic mucosa defines a two-variable signature enabling higher targeting specificity than either trigger independently. Mechanistically, ROS-responsive chemical linkages are incorporated into the hydrogel network alongside ionisable groups: thioketal bonds are cleaved by H_2O_2 through a peroxide-mediated hydrolysis mechanism; phenylboronate esters are oxidised by H_2O_2 to release phenol and borate; and ferrocene moieties cycle between Fe^{2+} and Fe^{3+} oxidation states in response to superoxide. Itaconic acid-acrylamide nanogels achieve dual-trigger functionality intrinsically: the carboxylic acid groups provide pH-triggered swelling (10-fold between gastric and colonic pH) while electron-rich vinyl and enone moieties in the IAc backbone scavenge superoxide through radical addition reactions — providing a ROS-scavenging activity five times greater than control formulations.

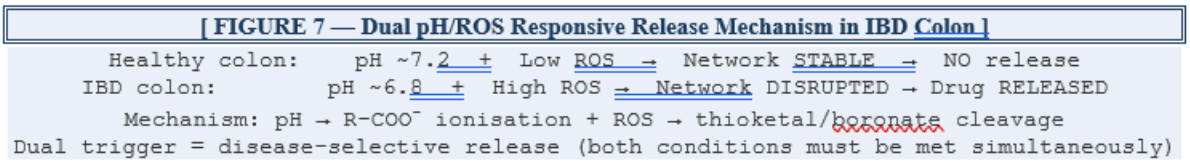

Figure 7. Mechanistic schematic of dual pH/ROS-responsive drug release in the IBD colonic microenvironment. In healthy colonic tissue, luminal pH is near-neutral (~7.2) and ROS concentrations are low — while pH may trigger partial ionisation, insufficient ROS prevents complete crosslink cleavage, maintaining network integrity. In actively inflamed IBD mucosa, both near-neutral pH (generating R-COO⁻ ionisation-driven swelling) and elevated H_2O_2 (cleaving thioketal or phenylboronate ester crosslinks) occur simultaneously, providing the dual trigger for network disintegration and biologic payload release specifically at the disease site. This pathology-selectivity principle improves the therapeutic index by preventing biologic release in non-inflamed colonic segments — a clinical advantage when limiting systemic biologic exposure is therapeutically important.

7.2 Enzyme-Responsive and AI-Assisted Design

Combining pH-triggered outer coating dissolution with enzymatic inner matrix degradation by colonic polysaccharidases creates systems requiring two simultaneous colonic conditions for release. The reliance on microbial enzymatic activity adds a disease-relevant adaptive dimension — dysbiotic IBD microbiota modulates enzyme availability, creating a pharmacokinetic profile that intensifies delivery as disease activity increases and enzyme diversity is restored. Machine learning QSPR models trained on polymer swelling datasets enable in silico prediction of swelling ratios for novel monomer combinations. Molecular dynamics simulations reveal that network heterogeneity rather than average mesh size is the dominant predictor of antibody diffusivity — a mechanistically important finding with direct crosslink density optimisation implications.

8. Characterisation Methodologies

Table 7 organises principal characterisation techniques, their outputs, and their significance for biologic hydrogel performance assessment.

Table 7. Characterisation methods for pH-responsive hydrogels loaded with biologic payloads.

Parameter	Technique(s)	Key Metrics	Significance for Biologic Hydrogel
pH-swelling response	Gravimetric swelling at pH 1.2, 4.5, 6.8, 7.4 / 37°C	ESR; swelling kinetics; transition threshold	Primary functional descriptor; ESR fold-change pH 7.4 vs 1.2 defines colon selectivity
Viscoelastic properties	Dynamic oscillatory rheology	G', G", gel point, shear-recovery kinetics	Confirms solid-like behaviour; G' predicts resistance to peristaltic disruption
Chemical structure	FTIR-ATR; ^{1}H NMR	Crosslink bond formation; polymer–drug H-bonding; residual monomer	Confirms crosslinking chemistry; reveals drug–polymer interaction; detects cytotoxic residuals
Crystallinity / thermal	XRD; DSC; TGA	Crystallinity index; Tg, Tm; degradation onset	Biologic amorphisation on encapsulation may alter

			stability; DSC Tm signals protein conformational state
Particle morphology	SEM (cryo-stage); AFM	Pore size; homogeneity; bead sphericity	Pore size vs biologic hydrodynamic radius governs diffusional release; cryo-SEM preserves swollen architecture
Particle size and charge	DLS; laser diffraction; zeta potential	Z-average diameter; PDI; ζ-potential at different pH	Size predicts mucosal penetration; pH-dependent size change confirms swelling
Biologic secondary structure	Far-UV CD; FTIR amide I/II	α-helix %; β-sheet %; random coil	Loss of α-helix or β-sheet indicates destabilisation affecting bioactivity
Biologic tertiary structure	Near-UV CD; Trp fluorescence; nanoDSF	Aromatic microenvironment; Tm; ΔTm vs reference	CDRs of antibodies reside in tertiary structure; Tm reduction >2°C signals relevant destabilisation
Aggregation state	SEC-MALS; SDS-PAGE non-reducing	Monomer fraction %; HMW aggregate content	Aggregates immunogenic and inactive; non-reducing SDS-PAGE reveals disulfide-bonded aggregates
In vitro drug release	USP Apparatus I/II; sequential pH change; biorelevant fluids	Cumulative release (%); rate constant; kinetic model n-value	Validates GI protection and colonic triggering; n-value from Korsmeyer-Peppas identifies diffusion vs swelling mechanism

The Korsmeyer-Peppas n-value obtained from in vitro release data provides mechanistic insight into whether diffusion or swelling dominates release — critical for selecting formulation optimisation strategy. An n-value below 0.45 suggests Fickian diffusion and indicates crosslink density can be reduced to accelerate release at colonic pH. An n-value approaching 0.89 suggests swelling-rate control and indicates that polymer hydration rate — governed by network ionisation kinetics — is the bottleneck. The nanoDSF thermal stability measurement (Tm) serves as an early warning indicator of biologic destabilisation during formulation: a Tm reduction greater than 2°C relative to the free protein benchmark signals clinically relevant conformational perturbation requiring reformulation.

9. Translational Challenges

Table 5 organises principal translational obstacles, their mechanistic root causes, and current or emerging countermeasures.

Table 5. Principal translational challenges in developing pH-responsive hydrogels for oral biologic delivery, with proposed solutions.

Translational Challenge	Mechanistic Root Cause	Current / Emerging Countermeasures
Acid-mediated biologic denaturation	Gastric pH 1.2–2.0 unfolds protein tertiary structure; RNA hydrolyses within seconds	Eudragit S100 outer coat; compact anionic network at gastric pH; amino acid excipient stabilisers; nanoparticle inner core
Luminal protease attack	Pepsin, trypsin, chymotrypsin, elastase and brush-border peptidases sequentially degrade protein and RNA	Dense hydrogel mesh steric exclusion; co-encapsulated protease inhibitors; PEGylation; MOF cage for siRNA
Premature small intestinal release	PAA swells above pH 4.5; alginate dissolves in phosphate-rich intestinal fluid	LBL multilayer with Eudragit S100 outer coat; higher-threshold synthetic copolymers
Short colonic mucosal contact	Peristalsis sweeps formulation past mucosa before adequate drug permeation	Thiolated chitosan mucoadhesion; FMGA (48-h retention); CD44-targeted HA; carbopol-chitosan coatings
Epithelial permeability barrier	Tight junctions restrict paracellular transport >~1 nm hydrodynamic radius	Chitosan tight junction opening; FcRn-mediated IgG transcytosis; CD44-mediated HA uptake
Natural polymer batch variability	Alginate M/G ratio, chitosan deacetylation, pectin esterification vary between batches	Tight supplier CoA specifications; in-process QC; shift to semi-synthetic analogues
Biologic stability during manufacture	Radicals oxidise amino acid residues; agitation aggregates proteins; heat unfolds domains	Post-gelation loading; trehalose/sucrose lyoprotectants; spray-freeze-drying; mild crosslinking
Regulatory / IVIVC complexity	Combination drug-device classification; no validated IVIVC for biologic hydrogels	Early pre-submission meetings; biorelevant dissolution media; mechanistic PK modelling

Biologic stability across the complete product lifecycle constitutes the most pervasive challenge. The Henderson-Hasselbalch equation explains why a biologic protein with a pI (isoelectric point) of 7.0 — near-neutral — is particularly vulnerable to aggregation during lyophilisation of an alginate matrix, as freeze-concentration effects raise local protein concentration while the amorphous polysaccharide matrix provides insufficient hydrogen-bonding stabilisation. Trehalose (0.5–1.0 M) and sucrose (0.2–0.5 M) act as preferential hydration agents — their hydroxyl groups preferentially interact with protein surfaces through water-replacement and water-structuring mechanisms, maintaining protein conformation during ice formation. Regulatory classification of combination drug-hydrogel products and the

absence of validated IVIVC frameworks remain the most significant non-technical barriers.

10. Clinical Translation Landscape

10.1 Current Clinical Evidence

Table 8 consolidates available clinical and late-preclinical evidence.

Table 8. Clinical-stage and advanced preclinical oral biologic delivery platforms relevant to colon-targeted pH-responsive hydrogel development.

Product / Platform	Biologic Type	Delivery Technology	Clinical Stage & Key Findings	Indication	Ref.
AVX-470 (Avaxia)	Bovine polyclonal anti-TNF-α IgG	Uncoated oral capsule	Phase IIa: tolerated to 3.5 g/day; faecal anti-TNF activity; mucosal healing signals	Ulcerative colitis	[26]
OPRX-106 (Protalix)	Recombinant anti-TNF fusion protein	Plant cell matrix; pH-sensitive release	Phase II: dose-dependent clinical response; detectable faecal drug concentrations	Ulcerative colitis	[5]
ORA-101 (research)	Anti-IL-6 antibody	pH/enzyme dual-sensitive Eudragit + amino acid core	Preclinical: superior mucosal delivery vs i.p. injection in DSS mouse; Phase I planned	Crohn's / UC	[5]
CALY-002 (siRNA)	siRNA targeting STAT3 / TL1A	LNP; oral LNP-hydrogel composite in development	Phase IIa (subcutaneous); oral hydrogel composite in early preclinical stage	IBD / CRC	[23]
FMGA exosome (academic)	MSC-derived exosomes (UMSC-EXO)	Fluidic microgel assembly (FMGA)	Preclinical: 48-h colonic retention; tight junction restoration in mouse and beagle models	IBD	[16]
Tamarind gum hydrogel (academic)	Model protein / anti-inflammatory cargo	β-CD-g-PMAA / tamarind gum crosslinked hydrogel	In vitro: <5% release pH 1.2; >94% at pH 7.4 over 30 h; biocompatible MTT assay	Colon delivery	[8]

The AVX-470 programme established feasibility of oral antibody dosing in humans and confirmed biologically active antibody reaching the colonic lumen. OPRX-106's Phase II success demonstrated dose-dependent clinical response and detectable faecal drug concentrations — quantifying the performance gap that pH-responsive hydrogel technology must close. A 100-fold improvement in mucosal bioavailability through Eudragit S100 + alginate protection would reduce required doses from grams to tens of milligrams, transforming economic feasibility.

10.2 FUTURE DIRECTIONS

Future developments include real-time physiological sensing for patient-specific adaptive release, living therapeutic cell carriers within pH-responsive matrices for continuous local biologic production, organ-on-chip models for human-relevant preclinical evaluation, and pharmacoeconomic strategies exploiting the high annual costs (USD 20,000–50,000) of parenteral biologic IBD therapy as economic justification for oral alternative development.

CONCLUSIONS

pH-responsive hydrogels represent a mechanistically well-grounded and experimentally validated approach to oral colon-targeted biologic delivery. The Donnan osmotic swelling mechanism, Flory-Rehner network thermodynamics, mesh-size-controlled macromolecular diffusion, and Korsmeyer-Peppas kinetic modelling together provide a rigorous quantitative framework for understanding, designing, and optimising these systems at the M.Pharm level. Polymer chemistry has evolved from single-component alginate and Eudragit® systems to dual-functional itaconic acid nanogels with intrinsic ROS scavenging, dynamic covalent Schiff base hydrogels with injectable and self-healing properties, and nanoparticle-in-hydrogel composites providing two-layer RNA protection. Formulation architecture advances — LBL multilayer beads, FMGAs with 48-hour mucosal retention, siRNA-MOF-alginate composites — have delivered therapeutic efficacy for anti-TNF-α antibodies, siRNA, and MSC-derived exosomes in preclinical IBD models.

Ten summary tables and seven schematic figure descriptions in this review consolidate the mechanistic, physicochemical, clinical, and translational knowledge base of the field. The principal translational challenges — biologic stability, natural polymer variability, scale-up manufacturing, combination product regulatory complexity, and absence of validated IVIVC frameworks — require sustained interdisciplinary effort. With continued collaboration across polymer science, pharmaceutical engineering, mechanistic pharmacokinetics, clinical gastroenterology, and regulatory science, pH-responsive hydrogels hold genuine promise as enabling platforms for the next generation of oral biologic therapies for colonic disease.

REFERENCES

1. Langer R, Peppas NA. Advances in biomaterials, drug delivery, and bionanotechnology. AIChE Journal. 2003;49(12):2990–3006.
2. Baral KC, Choi KY. Barriers and strategies for oral delivery of peptide and protein therapeutics. Pharmaceutics. 2025;17(3):397.
3. Pareek S, Soni R, Tripathi PK, Bhardwaj J. pH-responsive, ROS-scavenging and highly swellable nanogel for colon-targeted oral drug delivery. ACS Applied Nano Materials. 2024;7:18964–18978.
4. Suhail M, Shao YF, Vu QL, Wu PC. Designing pH-sensitive hydrogels for colon targeted drug delivery. Gels. 2022;8(3):155.

5. Yadav V, Chen L, Stauffer WR. Advances in colon-targeted drug technologies for oral delivery of biologics in IBD. Current Opinion in Gastroenterology. 2025;41(1):9–15.
6. Wang F, Li X, Zhao Q, Liu Q. Oral colon targeted protein delivery using alginate and chitosan nanospheres. Scientific Reports. 2025;15:4983.
7. Lei F, Zeng F, Yu X, et al. Oral hydrogel nanoemulsion co-delivery system treats IBD. Journal of Nanobiotechnology. 2023;21:275.
8. Devi A, Kumar R, Kaur P. Beta-cyclodextrin-based multifunctional carriers for colon-targeted drug delivery. Cancer Nanotechnology. 2025;16:32.
9. Bordbar-Khiabani A, Gasik M. Smart hydrogels for advanced drug delivery systems. International Journal of Molecular Sciences. 2022;23(7):3665.
10. Rabeh ME, Vora LK, Moore JV, et al. Dual stimuli-responsive delivery for colon-targeted drug release. Biomaterials Advances. 2024;157:213735.
11. Liu Q, Ma D, Cheng H, et al. pH-responsive nanogels from bioinspired comb-like polymers. Gels. 2025;11:806.
12. Gan X, Chen Y, Zhou M. Precision drug delivery in IBD via biomaterials. MedComm Biomaterials and Applications. 2025;4:e70022.
13. Renukadevi S, Kumar A, Shetty P. Gut-targeted nutraceutical delivery via microbiome-responsive interfaces. Food Bioengineering. 2025;3:e70024.
14. Hoang HT, Jo SH, Phan QT, et al. Dual pH-/thermo-responsive chitosan hydrogels for colon-targeted delivery. Carbohydrate Polymers. 2021;260:117812.
15. Zhuo Z, Guo K, Luo Y, et al. Dual-targeting bilirubin nanoparticles for intestinal epithelial regeneration. Theranostics. 2024;14(2):528–546.
16. Chen J, Li M, Zeng W, et al. Fluidic microgel assemblies for enhanced oral biologic delivery. Science Advances. 2025;11:eadv6994.
17. Manna K, Roy A, Pal S. Injectable pH-responsive biopolymeric hydrogel for site-specific delivery. ACS Applied Polymer Materials. 2025;7:4166–4176.
18. Patroklou G, Koumentakou I, Tsongas K, Bikiaris DN. pH-responsive hydrogels: recent advances. Polymers. 2025;17:1451.
19. Ibrahim MM, El-Leithy ES, Abdallah OY. pH-sensitive Eudragit coated beads for colon-specific delivery. Gels. 2023;9:264.
20. [20] Cao H, Wang T, Cheng M, et al. Dexamethasone microcrystals with pH-sensitive multilayers for IBD. Drug Delivery. 2018;25(1):2002–2012.
21. Gao M, Yang C, Wu C, et al. Hydrogel-MOF hybrids for oral siRNA delivery in ulcerative colitis. Journal of Nanobiotechnology. 2022;20:409.
22. Nalbadis A, Trutschel ML, Lucas H, et al. siRNA for sustained delivery from gellan gum hydrogels. Pharmaceutics. 2021;13:1546.
23. Liu X, Wu F, Tian Y, et al. Hydrogels for nucleic acid drug delivery. Advanced Healthcare Materials. 2024;13:e2401895.
24. Nugent SG, Kumar D, Rampton DS, Evans DF. Intestinal luminal pH in IBD. Gut. 2001;48(4):571–577.
25. Zhang C, Wang X, Xiao M, et al. Alginate/chitosan hydrogel for oral curcumin delivery. Materials and Design. 2022;221:110894.
26. Biosimilar and biologic therapy in IBD — challenges and strategies. PMC Review. 2025. PMC11972199.
27. Chen H, Islam W, El Halabi J. Innovative GI drug delivery systems. Frontiers in Bioscience. 2025;30:25281.

28. Martinez-Garcia FD, Fischer T, Hayn A, et al. Characterisation of hydrogel microarchitecture. Gels. 2022;8:535.
29. Chen S, Gao W, Ge P. Thermosensitive hydrogel with pectin microspheres for UC therapy. Biomacromolecules. 2024;25:6801–6813.
30. Cryan SA, O'Driscoll CM. Mechanistic studies on nonviral gene delivery to the intestine. Pharmaceutical Research. 2003;20(4):569–575.
31. Peppas NA. Analysis of Fickian and non-Fickian drug release from polymers. Pharmaceutica Acta Helvetiae. 1985;60(4):110–111.
32. Flory PJ, Rehner J. Statistical mechanics of cross-linked polymer networks. Journal of Chemical Physics. 1943;11(11):512–520.
33. Korsmeyer RW, Gurny R, Doelker E, Buri P, Peppas NA. Mechanisms of solute release from porous hydrophilic polymers. International Journal of Pharmaceutics. 1983;15(1):25–35.
34. Peppas NA, Sahlin JJ. A simple equation for the description of solute release. International Journal of Pharmaceutics. 1989;57(2):169–172.
35. Donnan FG. The theory of membrane equilibria. Chemical Reviews. 1924;1(1):73–90.

HOW TO CITE: Gautami Gangurde, Dr. Anil Jadhav, Dr. Atul Bendale, Prajwal Aher, pH-Responsive Hydrogels for Oral Colon-Targeted Delivery of Biologics: Recent Advances, Int. J. of Pharm. Sci., 2026, Vol 4, Issue 7, 665-687, https://doi.org/10.5281/zenodo.21156827